The magnetic and structural properties of the magnetic shape memory compound $Ni_2Mn_{1.44}Sn_{0.56}$

2006 J. Phys.: Condens. Matter 18 2249

(http://iopscience.iop.org/0953-8984/18/7/012)

INSTITUTE OF PHYSICS PUBLISHING JOURNAL OF PHYSICS: CONDENSED MATTER

J. Phys.: Condens. Matter **18** (2006) 2249–2259 doi:10.1088/0953-8984/18/7/012

The magnetic and structural properties of the magnetic shape memory compound $Ni_2Mn_{1.44}Sn_{0.56}$

P J Brown[1,2], A P Gandy[1], K Ishida[4], R Kainuma[4], T Kanomata[3], K-U Neumann[1], K Oikawa[4], B Ouladdiaf[2] and K R A Ziebeck[1]

[1] Department of Physics, Loughborough University, LE11 3TU, UK
[2] Institut Laue Langevin, BP 156, 38042 Grenoble, France
[3] Faculty of Engineering, Tohoku University, Tagajo 985-8537, Japan
[4] Department of Materials Science, Graduate School of Engineering, Tohoku University, Sendai 980-8579, Japan

Received 18 November 2005, in final form 14 December 2005
Published 2 February 2006
Online at stacks.iop.org/JPhysCM/18/2249

Abstract

Magnetization and high resolution neutron powder diffraction measurements on the magnetic shape memory compound $Ni_2Mn_{1.44}Sn_{0.56}$ have confirmed that it is ferromagnetic below 319 K and undergoes a structural phase transition which takes place at $T_M = 221$ K on cooling and 239 K on warming. The high temperature phase has the cubic $L2_1$ structure, $a = 5.973$ Å, with the excess manganese atoms occupying the 4(b) tin sites. In the cubic phase at 245 K the manganese moments at both sites were found to be ferromagnetically aligned. The magnetic moment at the 4(a) sites was 1.88(10) μ_B but it was only 0.53(18) μ_B/Mn at the 4(b) sites. The low temperature phase stable below T_M has an orthorhombic structure with space group $Pmma$ related to the cubic phase through a Bain transformation $\boldsymbol{a}_{ortho} = (\boldsymbol{a}_{cub} + \boldsymbol{b}_{cub})/2$; $\boldsymbol{b}_{ortho} = \boldsymbol{c}_{cub}$; $\boldsymbol{c}_{ortho} = (\boldsymbol{a}_{cub} - \boldsymbol{b}_{cub})$. The change in cell volume in the transition is only $\approx$0.5%, suggesting that the atomic moments are unchanged although the spontaneous magnetization drops significantly.

(Some figures in this article are in colour only in the electronic version)

1. Introduction

The characteristic property of shape memory materials is that once they are formed at the proper temperature they may be plastically deformed at a lower temperature, and on reheating will regain their original shape. This type of material is currently attracting a lot of interest since in recovering their shape the alloys can produce a displacement or a force or a combination of the two [1]. With currently available materials the transformation is not sufficiently rapid for many applications, or, as in the case of medical applications, a change of temperature is not appropriate. Considerable effort therefore is being made to find a system in which the phase transition can be controlled by a magnetic field at constant temperature. Ferromagnetic

shape memory alloys show large magnetic field induced strain due to the rearrangement of twin variants in the martensitic phase [2, 3]. In contrast with temperature induced effects the speed of shape change is not limited in this mechanism; such alloys therefore have potential for use as magneto-mechanical actuators. Several candidates have already been identified based on Ni_2MnGa [4–6], which has a Curie temperature of 376 K. At 200 K the alloy transforms from the cubic Heusler structure to one with an orthorhombic cell having one edge in common with the cubic cell. Although there is only a 1% volume change at T_M, there is considerable distortion of the cubic cell which becomes pseudo-tetragonal with $c/a = 0.93$. The field dependence of the preferred c-axis of the tetragonal variants gives rise to the large observed magnetostriction. Unfortunately the potential application of these particular materials is limited because they tend to be brittle and the phase change essential for shape memory behaviour occurs well below room temperature. Recently several new ferromagnetic shape memory compounds have been reported, one family of which is based on the ternary series $Ni_2Mn_{1-x}Z_{1+x}$ (Z = In, Sn and Sb), which have higher transition temperatures, some close to room temperature, and hence their potential for applications is significantly enhanced [7]. It has recently been shown [6] that the phase transition in the prototype ferromagnetic shape memory alloy Ni_2MnGa takes place by two successive shears on {110} planes in $\langle 1\bar{1}0\rangle$ directions and that the shape memory property arises from the consequent fixed orientation relationships between the martensitic twins and the high temperature cubic axes. In the Ni–Fe–Ga ferromagnetic shape memory system [8] on the other hand the martensitic phase has a different structure with $c/a > 1$: the transformation mechanism only involves one shear and the orientation relationships between the martensitic variants is different. A precise knowledge of the transformation process and the associated structures is therefore fundamental in establishing the mechanisms of shape memory behaviour. It is with that object in mind that the current study of one of the new compounds, $Ni_2Mn_{1.44}Sn_{0.56}$, has been undertaken.

2. Previous work

A combination of magnetization, x-ray and transmission electron microscopy measurements on $Ni_2Mn_{1.44}Sn_{0.56}$ indicates that the compound undergoes a structural phase transition around $T_M \approx 230$ K [7]. The austenite phase stable above T_M is reported to have the cubic Heusler $L2_1$ structure with $a \approx 5.9$ Å and below T_M in the martensitic phase an orthorhombic four-layered structure with lattice parameters $a \approx 4.3$ Å, $b \approx 2.87$ Å and $c \approx 8.4$ Å is formed. Although a similar structure occurs in the related compound Co_2NbSn [9] this is the first time it has been observed in a ferromagnetic shape memory compound. The relationship between the cubic austenite and orthorhombic cells is shown in figure 1. It has been suggested, on the basis of transmission electron microscopy measurements, that the phase transition takes place in two or three steps. Low field magnetization measurements suggest the presence of ferrimagnetic order in the martensitic phase. The twinning stress associated with the four-layered martensite is thought to be low, allowing easy displacement of the twin boundaries. In consequence it has been suggested that it should be possible to control the transition by applying a magnetic field. A partial phase diagram of the $Ni_2Mn_{1+x}Sn_{1-x}$ system has been proposed by Sutou *et al* [7] which is shown schematically in figure 2. In the range of composition studied, T_M decreases with increasing Sn content whereas the Curie temperature tends to increase. The vertical broken line is drawn at the composition of the alloy studied in the work presented here. At this composition three distinct phases are expected to occur, namely paramagnetic austenite, ferromagnetic austenite and ferromagnetic martensite. $Ni_2Mn_{1.44}Sn_{0.56}$ is therefore expected to undergo a martensitic phase transition in the ferromagnetic state at a temperature close to ambient.

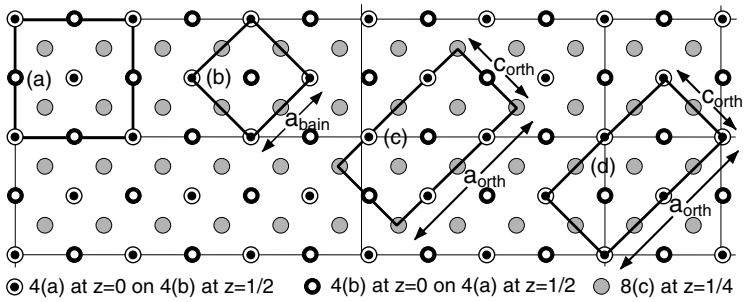

Figure 1. Projection on (001) of the ideal $L2_1$ Heusler structure showing (a) the $L2_1$ cell, (b) the body centred tetragonal cell following the Bain transformation; $c_{\mathrm{Bain}} = [001]_{\mathrm{cubic}}$, (c) the transformed orthorhombic cell which is referred to as a four-fold modulation in [7]; the *b*-axis is half of the cubic [001] axis and (d) the orthorhombic cell identified from the present work; the *b*-axis is the cubic [001] cell edge.

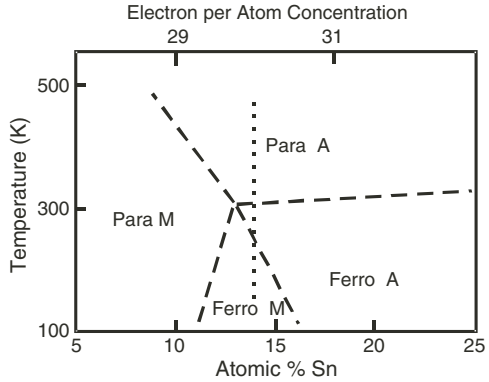

Figure 2. A schematic phase diagram of the $Ni_2Mn_{1+x}Sn_{1-x}$ system after [7].

3. Experimental details

A 20 g sample of $Ni_2Mn_{1.44}Sn_{0.56}$ was prepared by repeated melting of appropriate quantities of the constituent elements of 4 N purity in an induction furnace. The ingot was subsequently crushed to a particle size of less than 250 μm using a hardened steel pestle and mortar and the powder was then sealed in a quartz ampoule under a reduced argon atmosphere. The specimen was annealed for 2 days at 900 °C and then quenched into ice water. Subsequent x-ray diffraction measurements at room temperature confirmed that the resulting material was a single phase with the Heusler $L2_1$ structure, space group $Fm\bar{3}m$ with lattice parameter 5.793 Å.

Magnetization measurements were made using a SQUID magnetometer in fields up to 5.5 T and at temperatures between 5 and 350 K.

A detailed structural study was carried out using the high resolution neutron powder diffractometer D2b at the ILL in Grenoble. The powder specimen was contained in a thin walled vanadium can located in a closed cycle displex refrigerator mounted on the omega table of the diffractometer. Diffraction patterns were obtained at seven temperatures between 5 and 310 K, thus covering the range in which both the magnetic and structural phase transitions are expected to occur. The data were collected in steps of 0.05° in scattering angle 2θ, over the angular range $5° < 2\theta < 160°$ using a neutron wavelength of 1.59 Å.

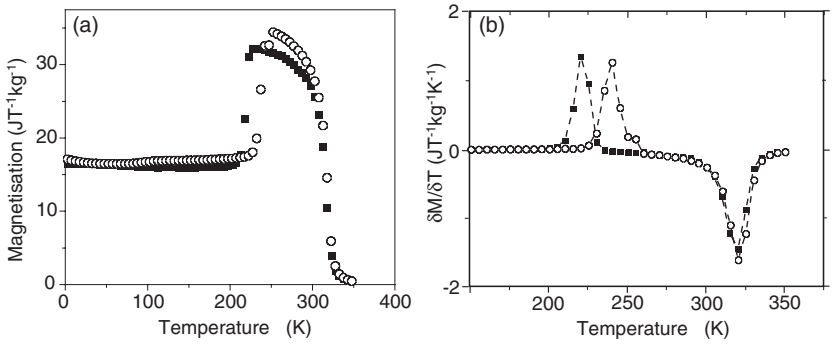

Figure 3. (a) The thermal variation of the magnetization of $Ni_2Mn_{1.44}Sn_{0.56}$ measured in an applied field of 0.1 T whilst heating ○, and cooling ■, between 5 and 350 K. (b) The differentials of the magnetization with respect to temperature which clearly indicate the structural and magnetic transition temperatures.

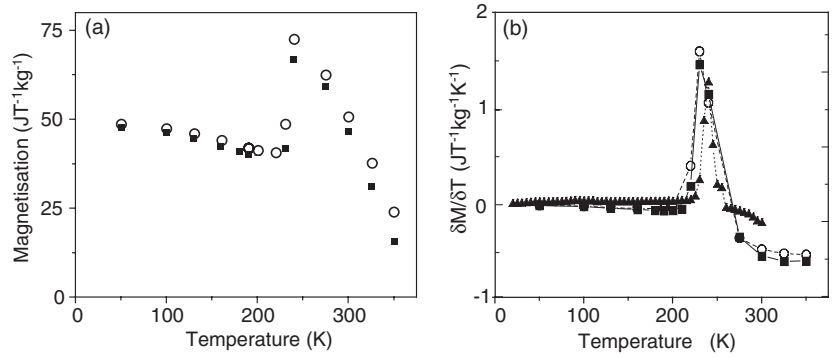

Figure 4. (a) The thermal variation of the magnetization of $Ni_2Mn_{1.44}Sn_{0.56}$ measured in applied fields of 3 T ■ and 5.5 T ○ whilst heating from 5 K. (b) The differentials of these curves together with that obtained at 0.1 T (filled triangles). They show that the structural transition temperature T_M does not change over this field range.

4. Results

4.1. Magnetization measurements

Initially the magnetization was measured in a field of 0.1 T during cooling from 350 to 5 K and then whilst heating back up to 350 K: both the magnetization values and their differentials with respect to temperature are shown in figure 3. Below ≈221 K on cooling and ≈239 K on heating the magnetization is essentially constant but at these temperatures there is an abrupt change. The behaviour is very similar to that reported at the martensitic transition in Ni_2MnGa [4]. It can therefore be assumed that these temperatures are those of the structural phase transition and that it has a hysteresis of 18 K. Measurements of the thermal variation of the magnetization whilst heating in fields of 3 and 5.5 T gave very similar results. The magnetization is shown in figure 4(a) and the differential curves are shown in figure 4(b). They show that there is negligible field dependence of T_M for fields up to 5.5 T, but confirm a significant fall in magnetization in the transition to the martensitic phase. The magnetic isotherms, shown in figure 5, have the characteristic form expected for a ferromagnet both above and below T_M. The spontaneous magnetization at 5 K, 47.32 J T^{-1} kg^{-1}, is significantly

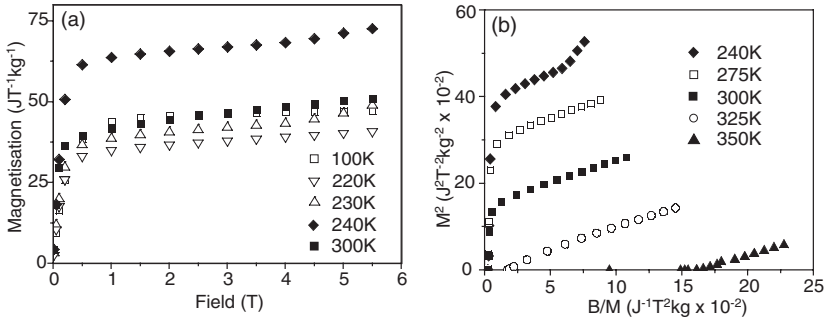

Figure 5. (a) Magnetic isotherms measured above and below the structural phase transition in $Ni_2Mn_{1.44}Sn_{0.56}$. (b) Some of the high temperature isotherms in the form of Arrott plots (M^2 versus B/M).

Table 1. A summary of the results of magnetization measurements on $Ni_2Mn_{1.44}Sn_{0.56}$.

Curie temperature, T_C	(K)	319(3)
Martensitic transition T_M on cooling	(K)	221(3)
Martensitic transition T_M on heating	(K)	238.8(3)
Spontaneous magnetization at 5 K	(J T^{-1} kg^{-1})	47.32(5)
Spontaneous magnetization at 245 K	(J T^{-1} kg^{-1})	62.30(5)
Magnetic moment per Mn atom at 5 K	(μ_B)	2.14(5)
Magnetic moment per Mn atom at 245 K	(μ_B)	2.82(5)

less than the value 62.3 J T^{-1} kg^{-1} observed in the austenite phase at 245 K. The thermal variation of the spontaneous magnetization in the martensitic phase has a smooth Brillouin like variation suggesting a stable magnetic configuration. Close to T_M the magnetic isotherms of figure 5 for 230 and 240 K show an upturn at the highest field values, indicating a transition to a state of higher magnetization. The upturn at 240 K is shown more clearly when the data are presented in the form of the Arrott plots (M^2 versus B/M) shown in figure 5(b). These also confirm the ferromagnetic transition at ≈319 K. An estimate of the spontaneous magnetization at 0 K in the absence of a magnetic phase transition at T_M has been made by comparing the magnetization in the austenite phase with that of the ferromagnetic parent compound Ni_2MnSn ($T_C = 360$ K) which retains the cubic $L2_1$ structure down to 5 K [10]. Assuming that the thermal dependences of the magnetization would be similar leads to a spontaneous magnetization for cubic $Ni_2Mn_{1.44}Sn_{0.56}$ at 5 K of ≈86 J T^{-1} kg^{-1}, corresponding to 4.1 μ_B per formula unit. This may be compared with the observed spontaneous magnetization 47.32 J T^{-1} kg^{-1} and moment per formula unit of 2.14 μ_B. A summary of the bulk magnetic properties of $Ni_2Mn_{1.44}Sn_{0.56}$ is given in table 1.

4.2. Neutron diffraction

The neutron powder diffraction pattern of figure 6 obtained at 310 K, just below the Curie temperature ($T_C = 319$ K), shows 19 strong Bragg reflections all of which could be indexed on the $L2_1$ fcc lattice. A profile refinement of the scattered intensity confirmed that the specimen was highly ordered in the $L2_1$ structure. Since the coherent nuclear scattering amplitudes of the three constituents (Ni 10.3, Mn −3.73, Sn 6.1 fm) are very different from one another it was possible to determine the occupancies of the three sites. This confirmed that the excess manganese atoms occupy the vacant tin sites. A statistical χ^2 test was applied to the fits

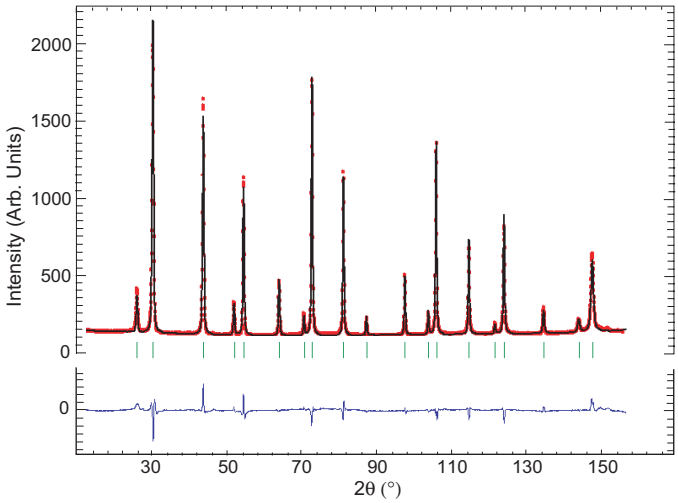

Figure 6. The neutron powder diffraction pattern of $Ni_2Mn_{1.44}Sn_{0.56}$ at 310 K. The plotted points show the observed counts and the full curve is the calculated profile. The inset at the bottom is the difference between the observed and calculated patterns. The calculated positions of the reflections are shown as vertical lines.

obtained with the powder patterns; it is defined by

$$\chi^2 = \frac{\sum_{\text{obs}} w(F_{\text{obs}} - F_{\text{calc}})^2}{N_{\text{obs}} - N_{\text{par}}} \qquad \text{with} \quad w = 1/\sigma(F_{\text{obs}})^2 \tag{1}$$

where N_{obs} is the number of observations, N_{par} the number of parameters and $\sigma(F_{\text{obs}})$ the estimated standard deviation of the observed structure factor F_{obs}. The results obtained in the refinement are given in table 2 and the calculated and difference diffraction patterns are shown in figure 6.

Cooling to 250 K made very little difference to the diffraction pattern apart from a change in the intensity of the low angle reflections consistent with the material becoming ferromagnetic. The most significant changes in intensity are observed for the $h + k + l$ odd reflections which are those with the smallest nuclear contribution. For these reflections the magnetic structure factor is given by $4f(hkl)(\mu_{4(a)} - \mu_{4(b)})$, where $f(hkl)$ is the Mn form factor and $\mu_{4(a)}$ and $\mu_{4(b)}$ are the magnetic moments at the 4(a) and 4(b) sites respectively. For the $h + k + l$ even reflections the increase in intensity was much smaller, amounting at most to a few per cent. In Ni_2MnGa and other compounds in the Ni_2MnZ series [10] the magnetic moment is predominantly due to manganese whilst nickel has only a small moment $\approx 0.3\ \mu_B$. In the profile refinement, therefore, a moment with a Mn^{2+} form factor was included for both the 4(a) and 4(b) sites, but no moment was associated in the first instance with the 8(c) sites. Initially the moments per manganese on the 4(a) and 4(b) sites were constrained to be identical but a significantly improved fit was obtained by allowing different sized moments. The relative orientation of the moments was also allowed to vary in the refinement but the best fit was found for the parallel configuration. The results are included in table 2 and the observed, fitted and difference patterns are shown in figure 7. These results show that there is no significant distortion of the paramagnetic Heusler structure as a result of ferromagnetic order. The sum of the moments on all three sites, 2.79(3) μ_B, is in good agreement with the value 2.82(5) μ_B obtained from magnetization measurements.

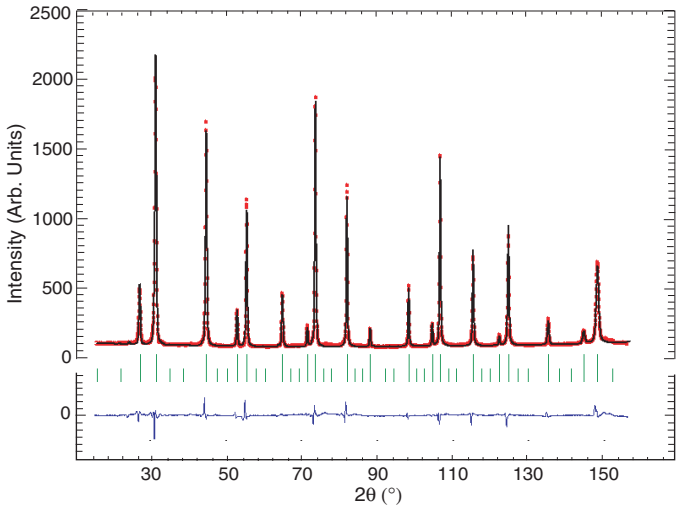

Figure 7. The neutron powder diffraction pattern of $Ni_2Mn_{1.44}Sn_{0.56}$ at 250 K, just above the structural transition, displayed in the same way as figure 6.

Table 2. Parameters of the cubic $L2_1$ and orthorhombic martensite structures of $Ni_2Mn_{1.44}Sn_{0.56}$ determined from the profile refinement of neutron powder patterns at 250 and 5 K.

Structure	Cubic $L2_1$ $Fm\bar{3}m$		Orthorhombic $Pmma$		
T (K)	250		5		
Cell (Å)[a]	$a = 5.967\,47(2)$		$a = 8.5837(2)$ $b = 5.6021(1)$ $c = 4.3621(1)$		
Atom	Site	μ (μ_B)	Site	y	z
Ni	8(c) $\frac{1}{4}\frac{1}{4}\frac{1}{4}$	0.33(4)	4(h) $0y\frac{1}{2}$	0.2495(7)	
			4(k) $\frac{1}{4}yz$	0.2485(8)	0.0913(3)
Mn	4(a) 000	1.88(10)	2(a) 000		
			2(f) $\frac{1}{4}\frac{1}{2}z$		0.574(2)
0.44Mn	4(b) $\frac{1}{2}\frac{1}{2}\frac{1}{2}$	0.53(18)	2(b) $0\frac{1}{2}0$		
+0.56Sn			2(e) $\frac{1}{4}0z$		0.562(4)

[a] Relative to a neutron wavelength taken as 1.59 Å.

At 225 K, close to the structural phase transition ($T_M \approx 221$ K) indicated by the magnetization measurements, the diffraction pattern became more complex. New Bragg peaks appeared but the dominant reflections could still be identified with the cubic austenite phase, showing that it had only partially transformed. At 200 K the transformation was complete, all the cubic reflections had disappeared and only peaks associated with the transformed phase were left. The appearance of the diffraction patterns then remained the same down to 5 K. There was no difference in either the peak shapes or peak widths of the Bragg reflections belonging to the austenite and martensite phases. At 225 K a small hump in the background, centred at $2\theta \approx 27°$, appeared and persisted unchanged down 5 K. This indicates some degree of short range order which could be of magnetic origin.

The diffraction pattern measured at 5 K which contains no residual cubic component was used to determine the crystal structure of the martensitic phase. Initially an attempt was made to index the reflections using the orthorhombic cell and lattice parameters reported by

Sutou *et al* [7]. However, this cell did not account for all the observed reflections. This deficiency was overcome by doubling the length of the b axis and allowing slight changes in the lengths of the other axes. The values given in table 2 were found to give a good fit to the positions of all the peaks. A group–subgroup analysis indicated that the only space group derived from $Fm\bar{3}m$ compatible with this orthorhombic cell is $Pmma$, and this was found to predict all the observed reflections correctly. When the $\boldsymbol{a}$, $\boldsymbol{b}$ and $\boldsymbol{c}$ axes are chosen to be consistent with this space group (International Tables #51), the relationship between the cubic and orthorhombic cells is

$$\begin{aligned} \boldsymbol{a}_{\text{ortho}} &= \boldsymbol{a}_{\text{cub}} - \boldsymbol{b}_{\text{cub}} \\ \boldsymbol{b}_{\text{ortho}} &= \boldsymbol{c}_{\text{cub}} \\ \boldsymbol{c}_{\text{ortho}} &= (\boldsymbol{a}_{\text{cub}} + \boldsymbol{b}_{\text{cub}})/2. \end{aligned} \tag{2}$$

The atomic sites of the orthorhombic structure are given in table 2.

An initial refinement of the nuclear structure at 5 K was made using the high angle diffraction data ($2\theta > 60°$) and the orthorhombic cell with atom sites as given in table 2. The results of this refinement were then used to generate a diffraction pattern for the full angular range covered in the experiment. This analysis showed that only one peak in the pattern, that made up of the 210 and 011 reflections, contained significant magnetic scattering. Furthermore, no additional reflections which might have purely magnetic origin were observed, confirming a $q = 0$ magnetic structure. For an orthorhombic structure it is possible, in principle, to determine both the magnitude of the moments and their orientations with respect to the three distinct crystallographic axes. However, the paucity of significant magnetic scattering makes such a complete analysis impracticable. The refinement of the 250 K data showed that the moments at the 4(b) site were small. Therefore in an initial refinement of the magnetic structure at 5 K magnetic moments were only assigned to the 2(a) and 2(f) sites. A series of collinear and canted models with zero propagation vector was tried. Although the magnetic contribution to the peaks was in general low, the absence of significant magnetic scattering in some of the low angle reflections, e.g. 100, places severe constraints on the moment direction. In all the models considered the magnetic scattering in the 210 and 011 reflections arises from a ferromagnetic component. The three models which gave the best agreement with the observations are presented in table 3, from which it may be seen that the mean moment per cell is very similar in all three models. The pattern fitted using model 1 in which ferromagnetic moments were constrained to be parallel to [100] is shown in figure 8 together with the difference between the observed and calculated profiles. Very similar fits were obtained for the other two models given in table 3. The magnetic contribution to the data was not sufficient to allow moment values to be refined for the Ni atoms or for the Mn atoms on the 2(b) and 2(e) sites.

A subsequent series of refinements was carried out for the data collected between 225 and 5 K. The lattice parameters obtained from the refinements and the corresponding cell volumes are plotted against temperature in figure 9. At 225 K only ≈16% of the sample was found to have transformed into the orthorhombic structure.

5. Discussion

The results reported in the previous section have confirmed the transformation sequence suggested by the vertical broken line in figure 2. The relationship between the unit cells of the two structurally different phases is illustrated in figure 1. The low temperature martensitic phase is derived from the cubic Heusler structure by a periodic displacement with propagation vector $(\frac{1}{2}\frac{1}{2}0)$ of the atoms in successive (110) planes along the $[1\bar{1}0]$ direction. This leads

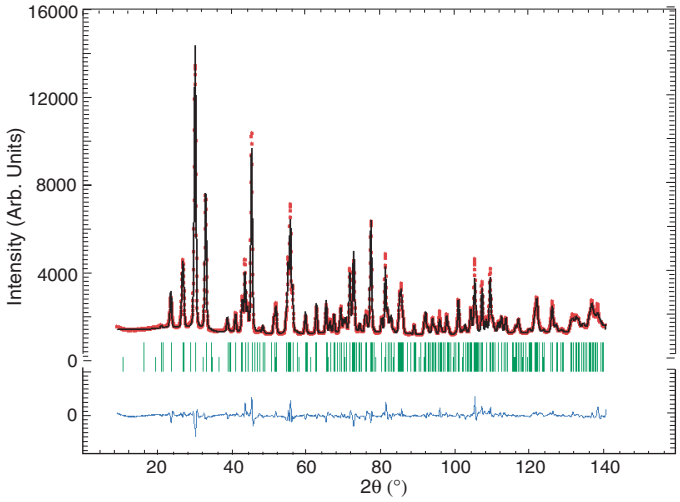

Figure 8. The neutron powder diffraction pattern of $Ni_2Mn_{1.44}Sn_{0.56}$ in the transformed phase at 5 K, displayed in the same way as figure 6.

Table 3. Magnetic structure models refined for $Ni_2Mn_{1.44}Sn_{0.56}$ at 5 K.

Model		1[a]	2[a]	3[a]	
Site		M_x (μ_B)	M_z (μ_B)	M_x (μ_B)	M_z (μ_B)
2(a)	000	2.9(2)	3.2(2)	0.94(15)	2.1(2)
	$\frac{1}{2}00$			−0.94(15)	2.1(2)
2(f)	$\frac{1}{4}\frac{1}{2}z$	2.6(2)	2.5(2)	0.49(14)	3.6(2)
	$\frac{3}{4}\frac{1}{2}z$			−0.49(14)	3.6(2)
χ^2		6.4	6.75	6.6	
R_B[b]		6.16	6.45	6.45	
R_{Mag}[b]		6.0	6.4	5.9	

[a] Model 1: moments fixed ∥ [100]. Model 2: moments fixed ∥ [001]. Model 3: moments confined to the (010) plane.
[b] R_B and R_{Mag} are the Bragg and magnetic agreement indices given by the FULPROF refinement.

to the orthorhombic unit cell space group $Pmma$ with $a_{ortho} = \sqrt{2}a_{cub}$, $b_{ortho} = a_{cub}$ and $c_{ortho} = a_{cub}/\sqrt{2}$; the orientation relationships are given by equation (2). The thermal evolution of the lattice parameters is shown in figure 9. Below T_M both a_{orth} and c_{orth} decrease slightly as the temperature is lowered whereas b_{orth} tends to increase. At T_M the maximum change in cell parameter is that of b_{orth} which, in the cubic phase, is a cell edge. Although the fractional change $b_{orth}/a_{cub} \approx 0.95$ the change in cell volume at T_M is only ≈0.5%. The displacements along $\boldsymbol{a}_{ortho}$ of the sublattices of Mn, Ni and Mn/Sn atoms in planes parallel to $\boldsymbol{c}_{ortho}$ are similar to one another and in phase. The modulation along x is approximately sinusoidal although from the results of the refinement in table 2 it can be seen that there are also significant atomic displacements in the y direction. The atomic positions are similar to those determined for the paramagnetic transformed phase of Co_2NbSn [9] which also has the $Pmma$ space group.

The use of neutron diffraction for the crystal structure determination of $Ni_2Mn_{1.44}Sn_{0.56}$ is particularly appropriate because of the large difference between the nuclear scattering lengths of Ni and Mn; additionally, low absorption allows large volumes (≃1 cm^3) to be probed. The

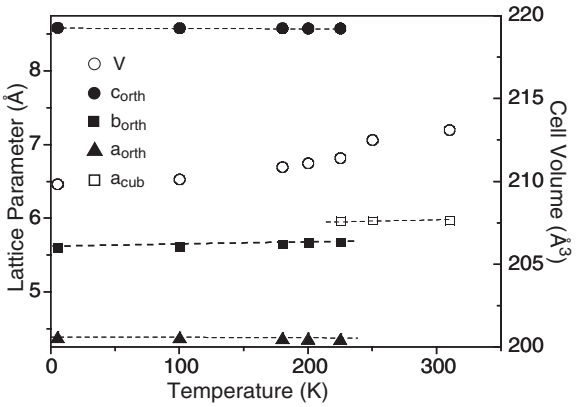

Figure 9. The temperature dependence of the lattice parameters and cell volume of $Ni_2Mn_{1.44}Sn_{0.56}$.

magnetic structure on the other hand is not so well determined since, for a ferromagnet, nuclear and magnetic scattering occur in the same reflections and the proportion of magnetic scattering is small. Above T_M the resultant magnetic moments on the 4(a) and 4(b) sites were found to be parallel to one another but the moment associated with Mn atoms on the 4(b) sites was significantly smaller (0.53(18) μ_B/Mn) than the value 1.88(10) μ_B found for the 4(a) sites. The magnetic isotherms above and below the structural phase transition have the characteristic form expected for a ferromagnet. Close to T_M, however, they suggest the onset of a metamagnetic transition consistent with a reorientation of the moments in high fields. This suggests that the reduction of ≈46% in the magnetization below T_M is not entirely the result of magnetic anisotropy in the orthorhombic structure and magnetostrictive alignment of the variants, but is due to some antiparallel alignment of moments. This is confirmed by the structure refinements below T_M in which no significant resultant moment on the 2(b) and 2(e) sites could be refined. The reduction may be due to incipient antiferromagnetic coupling between manganese atoms on the 4(b) sites of the austenite phase which is strengthened in the martensitic transition. Since these sites are only partially occupied by manganese no ordered antiferromagnetic structure is established. Such antiferromagnetic coupling could be the origin of the diffuse peak in the powder pattern corresponding to a d spacing of approximately one half of the separation in the ⟨101⟩ directions of the atoms on the 2(b) and 2(e) sites. A more complete refinement of the magnetic structure would require single crystal measurements. The manganese moments determined in $Ni_2Mn_{1.44}Sn_{0.56}$ are significantly smaller than those reported for alloys in the Ni_2MnZ series ordered in the $L2_1$ structure [10]. However, on the basis of polarized neutron measurements, manganese moments of a similar magnitude were reported in the austenite and martensitic phases of a partially disordered Ni_2MnGa crystal [15].

Magnetic order in Heusler alloys depends strongly on both the conduction electron concentration and the degree and type of atomic order [11, 12]. The exchange interactions are long range and of an indirect RKKY type. In the case of Ni_2MnSn the exchange interactions extend up to the seventh nearest neighbour [13]. Preliminary inelastic neutron scattering measurements on Ni_2MnGa suggest that a similar situation prevails [14].

$Ni_2Mn_{1.44}Sn_{0.56}$ is brittle and may be expected to have similar mechanical properties to Ni_2MnGa. The brittle nature of the compound and its transition temperature T_M, which is only slightly higher than that of Ni_2MnGa but still well below room temperature, is likely to limit any practical applications. One result probably associated with the brittle nature of the alloy

is the relatively small hysteresis of the transition, 18 K. The invariance in the shape and width of the Bragg peaks above and below T_M is also evidence that the martensitic phase does not support residual strain. All this is in contrast to the Co–Ni–Al and Co–Ni–Ga systems [16] which are ductile and have phase transitions close to room temperature.

The martensitic phase in $Ni_2Mn_{1.44}Sn_{0.56}$ is closely related to both the premartensitic and martensitic phases of Ni_2MnGa. All three have orthorhombic structures derived by periodic modulation of the $L2_1$ Heusler structure by shifts of atoms in 110 planes in $[1\bar{1}0]$ directions. In Ni_2MnGa the modulation vector is $(\frac{1}{3}\frac{1}{3}0)$ for the premartensitic phase and $(\frac{1}{7}\frac{1}{7}0)$ for the martensitic one. In $Ni_2Mn_{1.44}Sn_{0.56}$ there is no evidence of a premartensitic phase and the martensitic phase has propagation vector $(\frac{1}{2}\frac{1}{2}0)$. Although it is not possible to determine the transformation mechanism from powder data, the similarities with Ni_2MnGa suggest that the mechanism may be similar to the one found for that compound involving two distinct 110 shears [6]. By contrast in systems in which the martensitic phase is not related to the parent phase though a Bain transformation, a different mechanism has been found [8].

References

[1] *Proc. SMART 2000 (Sendai, Japan)* 2000
[2] OHandley R C 1998 *J. Appl. Phys.* **83** 3263
[3] Murray S J, Farinelli M, Kantner C, Haung J K, Allen S M and OHandley R C 1998 *J. Appl. Phys.* **83** 7297
[4] Webster P J, Ziebeck K R A, Town S L and Peak M S 1984 *Phil. Mag.* **49** 295
[5] Brown P J, Crangle J, Kanomata T, Matsumoto M, Ouladdiaf B, Neumann K-U and Ziebeck K R A 2002 *J. Phys.: Condens. Matter* **4** 10159
[6] Brown P J, Dennis B, Crangle J, Kanomata T, Matsumoto M, Neumann K-U, Justham L M and Ziebeck K R A 2004 *J. Phys.: Condens. Matter* **16** 65
[7] Sutou Y, Imano Y, Koeda N, Omori T, Kainmura R, Ishida K and Oikawa K 2004 *Appl. Phys. Lett.* **85** 4358
[8] Brown P J, Neumann K-U and Ziebeck K R A 2004 *ILL Report 2004*
[9] Neumann K-U, Kanomata T, Ouladdiaf B and Ziebeck K R A 2002 *J. Phys.: Condens. Matter* **14** 1371
[10] Webster P J and Ziebeck K R A 1988 *Landolt Börnstein Neue Series* vol 19, p 75
[11] Webster P J and Ramadan M R I 1977 *J. Magn. Magn. Mater.* **5** 51
[12] Webster P J and Ramadan M R I 1979 *J. Magn. Magn. Mater.* **13** 301
[13] Noda Y and Ishikawa Y 1976 *J. Phys. Soc. Japan* **40** 690
[14] Brown P J, Neumann K-U and Ziebeck K R A 2004 *ILL Annual Report*
[15] Brown P J, Bagarwi A Y, Crangle J, Neumann K-U and Ziebeck K R A 1999 *J. Phys.: Condens. Matter* **11** 4715
[16] Brown P J, Ishida K, Kainuma R, Neumann K-U, Oikawa K, Ouladdiaf B and Ziebeck K R A 2005 *J. Phys.: Condens. Matter* **17** 1301